10th International Conference on Gas Hydrates (ICGH10)
Jun 21-26, 2020, Singapore

Gas hydrate saturation estimation from acoustic log data in the 2018 Alaska North Slope Hydrate-01 stratigraphic test well

Seth S. Haines[1*], Timothy S. Collett[1], Ray Boswell[2], Teck Kean Lim[3], Norihiro Okinaka[4], Kiyofumi Suzuki[4,5], Akira Fujimoto[4]
[1]*U.S. Geological Survey, Denver, Colorado, USA*
[2]*National Energy Technology Laboratory, U.S. Department of Energy, Morgantown, West Virginia, USA*
[3]*Toyo Engineering, Chiba, Japan*
[4]*Japan Oil, Gas, and Metals National Corporation, Chiba, Japan*
[5]*Currently at National Institute of Advanced Industrial Science and Technology, Japan*
[*]Corresponding author: shaines@usgs.gov

ABSTRACT

Completed in December 2018, the Alaska North Slope Hydrate 01 stratigraphic test well provides a wealth of logging-while-drilling (LWD) data for strata to below the base of gas hydrate stability (BGHS). This well is intended to be the first of three wells drilled for a long-term gas hydrate production test to be conducted by the National Energy Technology Laboratory, the Japan Oil, Gas and Metals National Corporation, and the U.S. Geological Survey (USGS). The Hydrate 01 stratigraphic test well confirmed the presence of gas hydrate in two sand reservoirs within the hydrate stability zone, indicating the suitability of this location for a long-term gas hydrate production test.

The USGS, using an effective-medium-theory rock-physics approach, has estimated gas hydrate saturations from compressional (P) and shear (S) wave log data acquired in the Hydrate 01 well. We assume that gas hydrate occurs as pore-filling load-bearing material (i.e., part of the grain matrix). For Unit D, approximately 500 feet above the BGHS, both P-wave and S-wave acoustic logs indicate moderate to high gas hydrate saturations with S-wave results slightly lower than those for P-waves. For Unit B, located just above the BGHS, we obtain moderate to high gas hydrate saturation estimates from both sonic logs. Our P-wave saturation estimates agree well with results from electrical-resistivity-based estimates, whereas estimates from nuclear magnetic resonance LWD data generally suggest 5 to 10 percent higher saturations; our S-wave results suggest lower saturations. These differences likely indicate complexities in the form of gas hydrate occurrence within the sediment pore space, potentially including differences between hydrate occurrence in Units B and D.

Keywords: gas hydrate, Alaska, sonic log data, saturation estimation

1. INTRODUCTION

Decades of research into natural gas hydrate systems have resulted in extensive knowledge regarding gas hydrate occurrence, its role in gas and fluid flow dynamics, its geomechanical implications, and its potential as a hydrocarbon resource. Among remaining uncertainties are three questions of particular interest: (1) in what morphology(ies) does gas hydrate exist in the pores of sediment; (2) how does the hydrate occurrence and morphology relate to the material's geologic properties; and (3) what exactly will be observed in a long-term (months or years) gas hydrate production scenario?

Addressing these questions, the National Energy Technology Laboratory, the Japan Oil, Gas and Metals National Corporation, and the U.S. Geological Survey (USGS) are conducting studies in preparation for a long-term gas hydrate production test on the Alaska North Slope (Okinaka et al., 2020). The first of three intended wells was drilled in December 2018, providing a wealth of logging-while-drilling (LWD) data (Figures 1 and 2) for strata to below the base of gas hydrate stability, described in detail by Boswell et al. (2020) and Collett et al. (2020). Sidewall cores were acquired in the borehole, and these provide a suite of valuable measurements on reservoir material properties (Yoneda et al., 2020). In addition, 3D vertical seismic profile data were acquired using fiber-optic distributed acoustic sensing (DAS) deployed in the Hydrate-01 well and surface vibrator sources, yielding high-resolution reservoir images (Lim et al., 2020). With these and other data, project scientists are developing a detailed reservoir model to help predict water and gas production and other key elements of the planned production test.

Supporting this work and broader goals of understanding gas hydrate occurrence in natural reservoirs, we have calculated gas hydrate saturation (S_{gh})

estimates using LWD data. In this contribution, we present results from effective-medium-theory-based sonic log data and compare with S_{gh} estimates from resistivity and nuclear magnetic resonance (NMR) logs to reveal reservoir properties and gas hydrate occurrence characteristics.

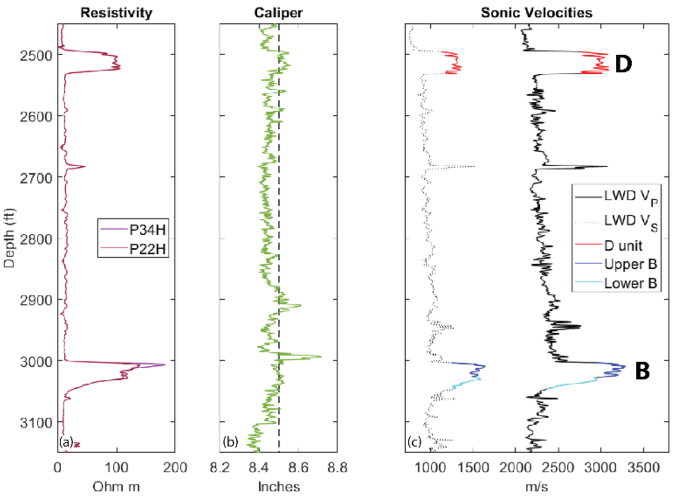

Figure 1. Selected logging-while-drilling (LWD) data from the stratigraphic test well. (a) Resistivity measurements P34H (deeper penetration) and P22H (shallower penetration), (b) caliper log, with dashed line indicating expected borehole diameter, and (c) P- and S-wave seismic velocities (V_P and V_S) with colored zones indicating reservoir sections (B and D).

2. DATA AND ANALYSIS

Borehole LWD data acquired in the stratigraphic test well include a full research-level log suite, described by Boswell et al. (2020) and Collett et al. (2020). Resistivity and sonic logs (Figure 1a and c) confirm the presence of gas hydrate in the reservoir section of Units B and D. Borehole conditions were generally very good, with minimal washout in the zone of interest (Figure 1b).

As a first step toward calculating gas hydrate saturation, we derived the fraction of sediment that is clay minerals, referred to as V_{shale}. We used a standard approach (e.g., Asquith and Krygowski, 2004), identifying end-member gamma-ray values corresponding with zero and 100% V_{shale}, (dashed lines in Figure 2a), and the relation I_{gr} = (gamma - $gamma_{min}$) / ($gamma_{max}$ - $gamma_{min}$). We then apply the standard relation for Tertiary rocks, $V_{shale} = 0.083*(2\text{^}(3.7*I_{gr}) - 1)$ to calculate V_{shale} (Figure 2b). Next, we calculate porosity (Figure 2b) from the density log, assuming grain density to be 2.695 g/cm^3 for both sand- and clay-rich sediments, based on analysis of sidewall cores (Yoneda et al, 2020).

We estimate S_{gh} from sonic logs (Figure 1) using the effective-medium-theory approach presented by Helgerud et al. (1999). We assume that gas hydrate occurs in a load-bearing morphology, following Helgerud et al. (1999), Lee and Collett (2001), and many other studies. We use elastic moduli as shown in Table 1, and we assume the critical porosity to be 0.37 and coordination number (number of contacts per grain) to be 9, following standard practices (e.g., Helgerud et al.,1999).

Plots in figure 2c and d show P-wave velocity (V_P) and S-wave velocity (V_S) calculated from LWD slowness logs, along with velocities estimated for a range of gas hydrate saturations. We expect only negligible gas hydrate in the non-reservoir sections of the well, such that the predicted V_P and V_S corresponding with S_{gh} = 0 should approximately match with the LWD-measured velocities. We find that this is true for V_P but less so for Vs, indicating that our selected physical properties and/or our rock-physics model is not entirely appropriate for this situation. Past authors (e.g., Lee and Collett, 2001) have noted that effective-medium-theory approaches can underpredict V_S, and we suggest that this may be the case for these Alaska data.

	Density (g/cm^3)	K (GPa)	G (GPa)
Sand	2.695	38	40
Clay	2.695	20.9	6.6
Gas hydrate	0.91	6.41	2.54
Pore water	1.02	2.4	0

Table 1. Material properties for effective-medium-theory calculations, modified from Helgerud et al. (1999), Lee and Collett (2011). K indicates the bulk modulus and G indicates the shear modulus.

For comparison with our sonic-derived S_{gh} estimates, we also present S_{gh} estimates from resistivity and NMR logs. We calculate S_{gh} from the resistivity data (specifically the P34H log shown in Figure 1) using a standard Archie equation approach (e.g., Lee and Collett, 2011). For the physical constants, we use a=1.6, m=2.1, and n=2.0, and we find little sensitivity of the calculated S_{gh} to adjustments of these values within reasonable ranges. Estimation of S_{gh} from NMR log data is based on the difference between the NMR- and density-derived porosity estimates. Because NMR is sensitive only to the liquid-water-filled porosity, the difference between these two porosity estimates corresponds with the gas-hydrate-filled porosity.

As is to be expected, all four gas hydrate estimates include uncertainty. One manifestation of this uncertainty is the estimation of spurious non-zero S_{gh} values in non-reservoir sedimentary sections (where we expect zero or near-zero S_{gh}), due to a variety of factors including physical property assumptions, LWD tool

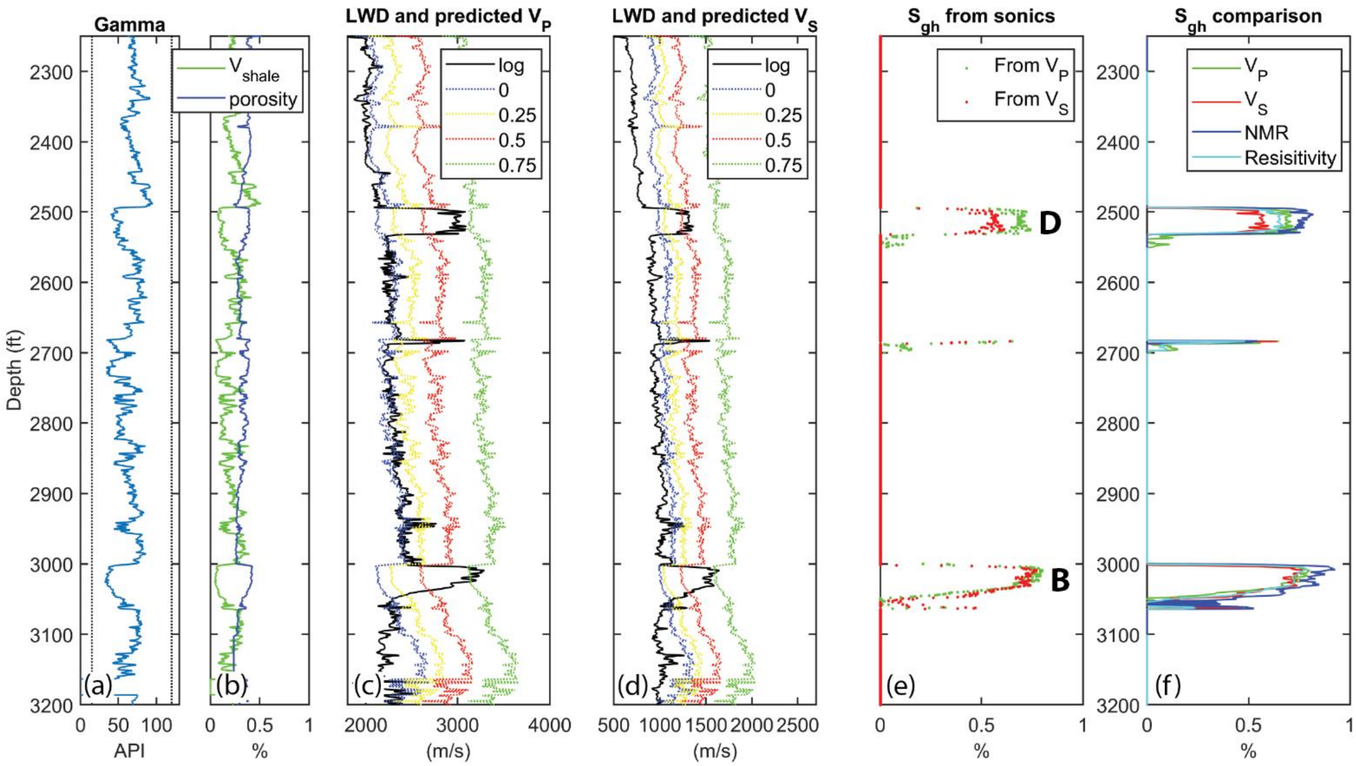

Figure 2. Gas hydrate saturation (S_{gh}) from sonic and other log data. (a) Logging-while-drilling (LWD) gamma ray log, (b) V_{shale} and porosity calculated as described in the text, (c) LWD-measured V_P (black line) and predicted V_P for S_{gh} values as indicated in the legend, (d) LWD-measured V_S (black line) and predicted V_S for S_{gh} values as indicated, (e) comparison of S_{gh} values estimated from V_P and V_S, (f) comparison of all four S_{gh} estimates. The reservoir portion of Units B and D are indicated with bold letters.

resolution differences, measurement imperfections, and rock physics considerations including those mentioned previously. To correct for these errors/uncertainties regarding exact parameters corresponding with S_{gh}=0, we have set to zero all S_{gh} values in non-reservoir strata.

3. RESULTS AND DISCUSSION

Measured LWD seismic velocities are shown as black lines in Figure 2c and d, for V_P and V_S, respectively. Along with these values are the velocities predicted by effective medium theory for S_{gh} values ranging from 0 to 75% of the pore space. Estimated S_{gh} values are shown in Figure 2e for the two sonic-based calculations. We observe high gas hydrate saturations, approaching 80%, in the reservoir portions of Units B and D. This in itself is a critical result, as it helps to confirm the suitability of these reservoir units for gas hydrate production testing. This topic is developed in greater detail by Boswell et al. (2020). In addition, comparison of the various S_{gh} estimates may provide insight regarding the reservoir and the measurement and estimation techniques.

We compare S_{gh} estimates in Figure 2e and f and observe that our four estimates are similar but not identical. Sonic-derived S_{gh} estimates are lower than those from other methods, and NMR-derived estimates are the highest. Among the four estimates, the resistivity-based estimate may be viewed as the most robust, due to the lack of significant sensitivity to any of the assumed parameters. In addition, the generally good agreement between the V_P-derived and resistivity-derived S_{gh} estimates lends confidence to those values. The NMR-derived S_{gh} estimates are calculated using our current best result for NMR-derived water-filled-porosity, but the NMR data processing is not yet finalized.

We observe that estimates from V_S are lower than those from V_P, and particularly so for the Unit D reservoir. This is at least partly related to the non-optimal fit of the S_{gh}=0 V_S estimate (blue line in Figure 2d) to the LWD V_S (black line), but it may also suggest that the hydrate morphology (pore-filling versus load-bearing versus cementing) differs between the reservoir portions of Units B and D. Investigating this further, we plot LWD-measured V_P versus V_S in Figure 3, for data from the two reservoir zones. In this plot, we distinguish the upper, high-quality portion of the B unit from the lower portion of that reservoir (as shown in Figure 1). In the crossplot, we observe a clear separation between these three sets of points. A number of factors may contribute to this distribution, including the fact that the reservoirs exist at different depths below ground surface, but the impact of these is expected to be minimal.

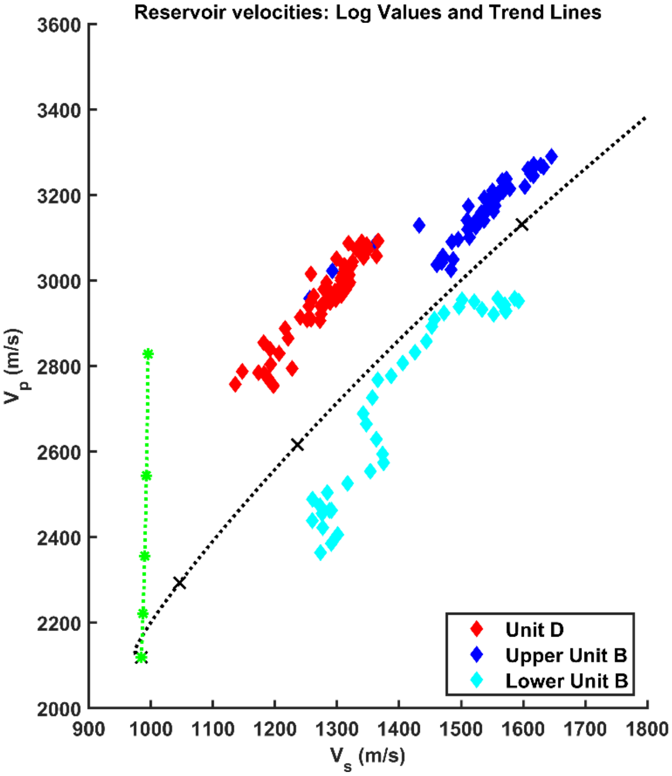

Figure 3. Crossplot of V_P versus V_S sonic log values for the hydrate-bearing reservoir units. Dashed green line shows values predicted for 0 to 100% gas hydrate saturation for a pore-filling morphology. Dashed black line shows values predicted for a load-bearing model.

Another factor, possibly a significant one, influencing the observed grouping is the morphology of each hydrate occurrence. For reference, we show trend lines for the following possible hydrate morphologies: (1) pore-filling (hydrate in pores, not impacting the stiffness of the grain matrix) and (2) load-bearing (hydrate adding stiffness to the grain matrix via grain contact but not cementing grains to one another). We observe that all three groups of V_P/V_S points plot around the load-bearing trend line. However, relative to the Unit B reservoir, the velocities for the Unit D reservoir plot nearer to the pore-filling trend line; this may suggest a somewhat different morphology possibly including a small component of pore-filling hydrate. We also note that the upper and lower Unit B reservoir groups show somewhat different characteristics, with the lower B group showing higher V_S relative to V_P. This could indicate hydrate in a more cementing morphology, but we suggest instead that this trend may be attributed to the observation that the lower part of Unit B reservoir possibly contains a greater clay fraction. Further emphasizing the different behavior of the reservoir zones, we observe in crossplots of V_P versus porosity and V_S versus porosity (Figure 4) that Unit D and the upper part of Unit B show greater separation in the V_S - porosity crossplot than in the V_P - porosity plot.

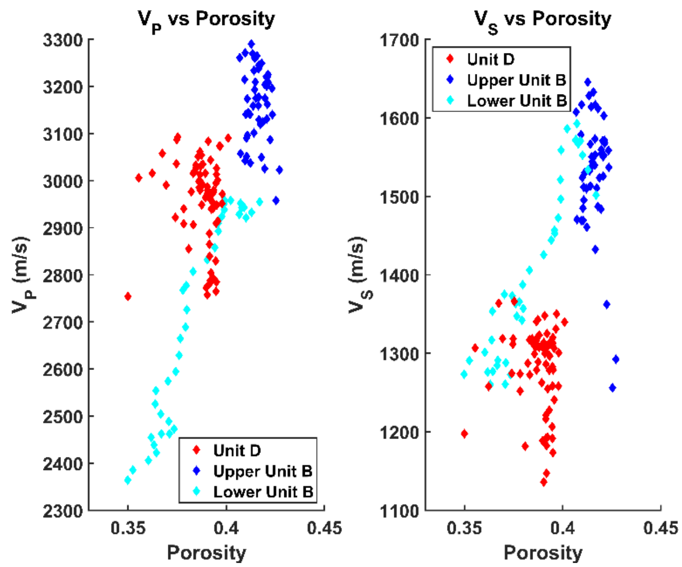

Figure 4. Crossplot of V_P (left) and V_S (right) sonic log values versus porosity values (calculated from the density log) for the primary reservoir units, as indicated.

4. CONCLUSIONS

Analysis of LWD borehole data from the Alaska North Slope gas hydrate stratigraphic test well confirms the presence of high concentrations of gas hydrate in the reservoir portions of Units B and D. Gas hydrate saturations as high as 80%, along with other reservoir characteristics, establish these reservoirs as being well suited to a long-term gas hydrate production test. Analysis of LWD sonic velocities V_P and V_S suggests the possibility that gas hydrate morphology may differ somewhat between the Unit B and D reservoirs, an inference with important implications regarding the formation of gas hydrate in reservoir strata, and regarding reservoir behavior under production conditions.

5. ACKNOWLEDGEMENTS

We thank all members of the Alaska North Slope Gas Hydrate Production Test science team for their contributions to this work. The project appreciates financial and technical support from the U.S. Department of Energy National Energy Technology Laboratory, Ministry of Economy, Trade and Industry (METI) Japan, MH21-S R&D consortium, the U.S. Geological Survey

Energy Resources Program, Toyo Engineering Corporation, and Japan Oil Engineering Co.

6. REFERENCES

Asquith, G., and D. Krygowski, 2004, Basic Well Log Analysis: AAPG Methods in Exploration 16, p.31-35

Boswell, R., Collett, T., Suzuki, K., Yoneda, J., Haines, S., Okinaka, N., Tamaki, M., Crumley, S., Itter, D., Hunter, R., 2020. Alaska North Slope 2018 Hydrate-01 Stratigraphic Test Well: Technical Results, Proc. ICGH-10, Singapore.

Collett, T., Okinaka, N., Wakatsuki, M., Boswell, R., Marsteller, S., Minge, D., Crumley, S., Itter, D., Hunter, R., 2020, Design and operations of the Hydrate-01 Stratigraphic Test Well, Alaska North Slope, Proc. ICGH-10, Singapore.

Helgerud, M., Dvorkin, J., Nur, A., Sakai, A., Collett, T., 1999, Elastic-wave velocity in marine sediments with gas hydrates: Effective medium modeling, Geophysical Research Letters, v. 26, 2021-2024.

Lee, M., Collett, T., 2001, Elastic properties of gas hydrate-bearing sediments, Geophysics, v. 66, 763-771.

Lee, M., Collett, T., 2011, In-situ gas hydrate saturation estimated from various well logs at the Mount Elbert Gas Hydrate Stratigraphic Test Well, Alaska North Slope, Marine and Petroleum Geology, v. 28, 439-449.

Lim, T.K., Fujimoto, A., Kobayashi, T., 2020. DAS-3DVSP data acquisition at 2018 Stratigraphic Test Well (Hydrate-01). Proc. ICGH-10, Singapore.

Okinaka, N., Boswell, R., Collett, T., Yamamoto, K., Anderson, B., 2020, Progress toward the establishment of an extended duration gas hydrate reservoir response test on the Alaska North Slope, Proc. ICGH-10, Singapore.

Yoneda, J., Jin, Y., Muraoka, M., Oshima, M., Suzuki, K., Walker, M., Westacott, D., Ohstuki, S., Kumagai, K., Collett, T., Boswell, R., Okinaka, N., 2020, Petrophysical and geomechanical properties of gas hydate0bearing sediments recovered from Alaska North Slope 2018 Hydrate-01 Stratigraphic Test Well, Proc. ICGH-10, Singapore.